6 hr tide seen in sporadic E layers

Jacobi, Ch.[+], Arras, C.[*]

+) Institute for Meteorology, Universität Leipzig, Stephanstr. 3, 04103 Leipzig, E-Mail: jacobi@uni-leipzig.de
**) German Research Centre for Geosciences GFZ, Potsdam*

Summary: The GPS radio occultation technique is used to study sporadic E (E_s) layer plasma irregularities of the Earth's ionosphere on a global scale using COSMIC/FORMOSAT-3 satellite constellation GPS signal-to-noise ratio (SNR) profiles. The maximum deviation from the mean SNR is attributed to the height of the E_s layer. E_s are produced by ion convergence due to vertical wind shear in the presence of a horizontal component of the Earth magnetic field, while the wind shear is provided mainly by solar tides. Indeed, close correlation between E_s and wind shear phases have already been found for the semidiurnal and terdiurnal tidal components. Here, we present the global distribution of quarterdiurnal (QDT) signatures in E_s occurrence rates. We find that, in accordance with upward energy flux, negative vertical phase gradients of QDT E_s signatures are observed. The maximum signal of QDT E_s is found at altitudes above 100 km. In the southern hemisphere, maximum QDT E_s occurrence rates are found in winter and during equinoxes. In the northern hemisphere, however, at altitudes above 100 km strong QDT activity is also visible.

Zusammenfassung: Die GPS-Radiookkultationstechnik wird verwendet, um ionosphärische Plasmairregularitäten in Verbindung mit sporadischen E- (E_s) Schichten auf globaler Skala zu untersuchen. Verwendet werden Signal-Rauschverhältnis- (SNR-) Profile. Die maximale Abweichung vom mittleren SNR wird der Höhe der E_s-Schicht zugeordnet. E_s werden durch Ionenkonvergenz aufgrund von vertikaler Windscherung in Anwesenheit einer horizontalen Komponente des Erdmagnetfeldes hervorgerufen, wobei die Scherung hauptsächlich durch solare Gezeiten verursacht wird. Tatsächlich wurden schon früher deutliche Übereinstimmungen zwischen dem Auftreten von E_s und den Phasen der halb- und dritteltägigen Gezeiten gefunden. Hier stellen wir die globale Verteilung der vierteltägigen (QDT) Signaturen in E_s-Auftretensraten vor. Es zeigt sich dass, in Übereinstimmung mit einem aufwärts gerichteten Energietransport, negative vertikale Phasengradienten der QDT in E_s auftreten. Die maximale Auftretenswahrscheinlichkeit liegt bei Höhen oberhalb von 100 km. Auf der Südhemisphäre fällt das Maximum der QDT in E_s-Auftretensraten in den Winter, während auf der Nordhemisphäre oberhalb von 100 km auch im Sommer starke QDT-Aktivität zu verzeichnen ist.

1. Introduction

The dynamics of the lower thermosphere are strongly influenced by atmospheric waves, including the solar tides with periods of a solar day, and its harmonics. Their wind amplitudes usually maximise around or above 120 km. In these regions, tidal amplitudes are of the order of magnitude of the mean wind. As a result, the solar tides drive the global circulation and more accurate knowledge of their spatial and temporal distribution leads to a better understanding of the wind fields in the lower thermosphere. Shorter period waves often have smaller amplitudes, so that in the past mainly the diurnal tide (DT), the semidiurnal tide (SDT), and also the terdiurnal tide (TDT) have been investigated. The quarterdiurnal tide (QDT), however, although it also forms an integral part of the middle and upper atmosphere dynamics, has attained much less attention, mainly due to its smaller amplitude. While, for example, near the surface the 6 hr-oscillation at times can be a major component e.g. in barographic records (e.g., Warburton and Goodkind, 1977), the amplitude in the mesosphere and lower thermosphere (MLT) is generally substantially smaller than those of the DT, SDT and also of the TDT. Consequently, only few attempts to determine the QDT characteristics from radar or satellite observations have been made so far. Examples of QDT analyses from radar observations have been presented by Smith et al. (2004) and Jacobi et al. (2017), and modelling of the QDT has also been made by Smith et al. (2004).

Earlier than in MLT winds or satellite observations, 6-hr tidal signatures have been observed in lower ionospheric sporadic E (E_s) parameters (Tong and Matthews, 1988; Morton et al., 1993). E_s layers are thin clouds of accumulated plasma, which occur primarily at midlatitudes and maximise during summer. They are generally formed at altitudes between 90 km and 120 km, i.e. in the lower thermosphere and the lower ionospheric E region. According to wind shear theory (Whitehead 1961) the process of E_s formation is an interaction between the Earth's magnetic field, the ion concentration, and the vertical wind shear. Neglecting diffusion, the vertical velocity component of the neutral gas, and the electric force, the vertical ion drift w_I may be written as (see Fytterer et al., 2014):

$$w_I = \frac{r \cdot \cos I}{1 + r^2} U - \frac{\cos I \cdot \sin I}{1 + r^2} V \,, \tag{1}$$

where U and V are the zonal and meridional wind components of the neutral gas, while I is the inclination of the Earth's magnetic field. The parameter $r = \nu/\omega$ describes the ratio of the ion-neutral gas collision frequency ν and the gyro frequency ω given by $\omega = eB_0/m_I$. Here, e is the elementary charge, B_0 is the total intensity of the Earth's magnetic field, and $\underline{m_I}$ is the ion mass. Note that in Eq. (1), in contrast to the usual notations in literature, Cartesian coordinates x, y, and z are used, pointing eastward, northward and upward, respectively. Considering that $r >> 1$ below ~115 km (Bishop and Earle, 2003), the zonal wind component is much more efficient in causing vertical plasma motion than the meridional wind component. Consequently, the second term of Eq. (1) may be neglected in the lower E region, and therefore negative vertical zonal wind shear primarily leads to the formation of E_s. Note that Eq. (1) holds only for magnetic midlatitudes (about 20° - 70°), where electric forces can be neglected.

Assuming that solar tides are the main source of the vertical wind shear, frequently providing larger vertical gradients than the background wind, tide-like structures are expected in E_s occurrence rates. Actually, the SDT and DT are generally accepted to be the major driver of E_s (Mathews, 1998), leading to the reproduction of downward moving tidal signatures e.g. in E_s ionosonde registrations (e.g. Haldoupis et al., 2006). By combining Global Positioning System (GPS) registrations and radar wind measurements, Arras et al. (2009) have shown that E_s occurrence frequencies actually maximize when the zonal wind shear provided by the SDT is negative. More recently, Fytterer et al. (2013, 2014) found a clear correlation between midlatitude radar zonal wind shear and E_s for the 8-hr component also, leading to the conclusion that not only DT and SDT, but TDT as well contributes to E_s formation. However, the 6-hr component has not yet been analysed in detail from GPS radio occultation (RO) observations, which motivates us to search for the QDT signature in Es occurrence rates (OR) derived from RO.

Therefore, in this paper we analyse the quarterdiurnal oscillation seen in E_s, obtained from GPS RO measurements by the FORMOsa SATellite mission-3/Constellation Observing System for Meteorology, Ionosphere and Climate (FORMOSAT-3/COSMIC). The paper is organised as follows. In section 2 the E_s detection is briefly described, while the QDT analysis from E_s OR is described in section 3. In section 4, the global distribution of the OR QDT signature is presented, and section 5 concludes the paper.

2. Analysis of sporadic E from COSMIC/FORMOSAT-3 radio occultations

The FORMOSAT-3/COSMIC constellation consists of six low-Earth orbiting (LEO) microsatellites which orbit the Earth at an initial altitude of ~800 km. The satellites perform RO measurement in both the neutral atmosphere and the ionosphere (Anthes et al., 2008). During an occultation, signals of rising or setting GPS satellites are received by a LEO satellite. While the signals pass Earth's atmosphere they are modified by atmospheric conditions, in particular ionospheric electron density, causing refraction and degradation of the GPS waves. More detailed information on the principles of the RO technique is given by Hajj et al. (2002) and Kursinski et al. (1997).

The method to derive E_s information from RO signals has been described in Arras and Wickert (2017). In brief, for our investigations, we use the Signal-to-Noise ratio (SNR) profiles of the GPS phase measurements. The SNR is very sensitive to height dependent changes in the electron density as they occur within an E_s layer. These vertically small variations in the electron density lead to phase fluctuations of the GPS signal which can be observed as a change of the signal power at the receiver (Hajj et al., 2002).

In order to avoid influences from the different basic signal power values on the further data treatment, every SNR profile is normalized first. In absence of ionospheric disturbances the SNR free-space value is almost constant at altitudes above 35 km. The SNR standard deviation profile is considered to include a disturbance in case it exceeds an empirically found threshold of 0.2. If large standard deviation values are concentrated within an altitude range of less than 10 km, it is assumed that the respective SNR profile includes the signature of an E_s layer. The height where the SNR value has the

strongest deviation from the mean of the SNR profile is assumed to be the altitude of the E_s layer.

Figure 1 shows 2007-2016 mean E_s occurrence rates (OR). OR have been calculated as the number of E_s within a 10° latitude and 10 km height window, divided by the number of RO in the respective latitude window. Figure 1 shows seasonal means for December–February (DJF), March–May (MAM), June–August (JJA) and September–November (SON). Maximum OR are found slightly above 100 km. OR maximise in summer. The summer maximum is more pronounced in the northern hemisphere, which is due to the South Atlantic Anomaly and the weaker magnetic field there, so that southern hemisphere summer OR are smaller than northern hemisphere ones. Near the equator, E_s OR are small, owing to the horizontal magnetic field at the magnetic equator, which does not allow electrons to follow the vertically moving ions, which results in low E_s OR there (e.g. Arras et al., 2008, 2010, 2013; Arras and Wickert, 2017).

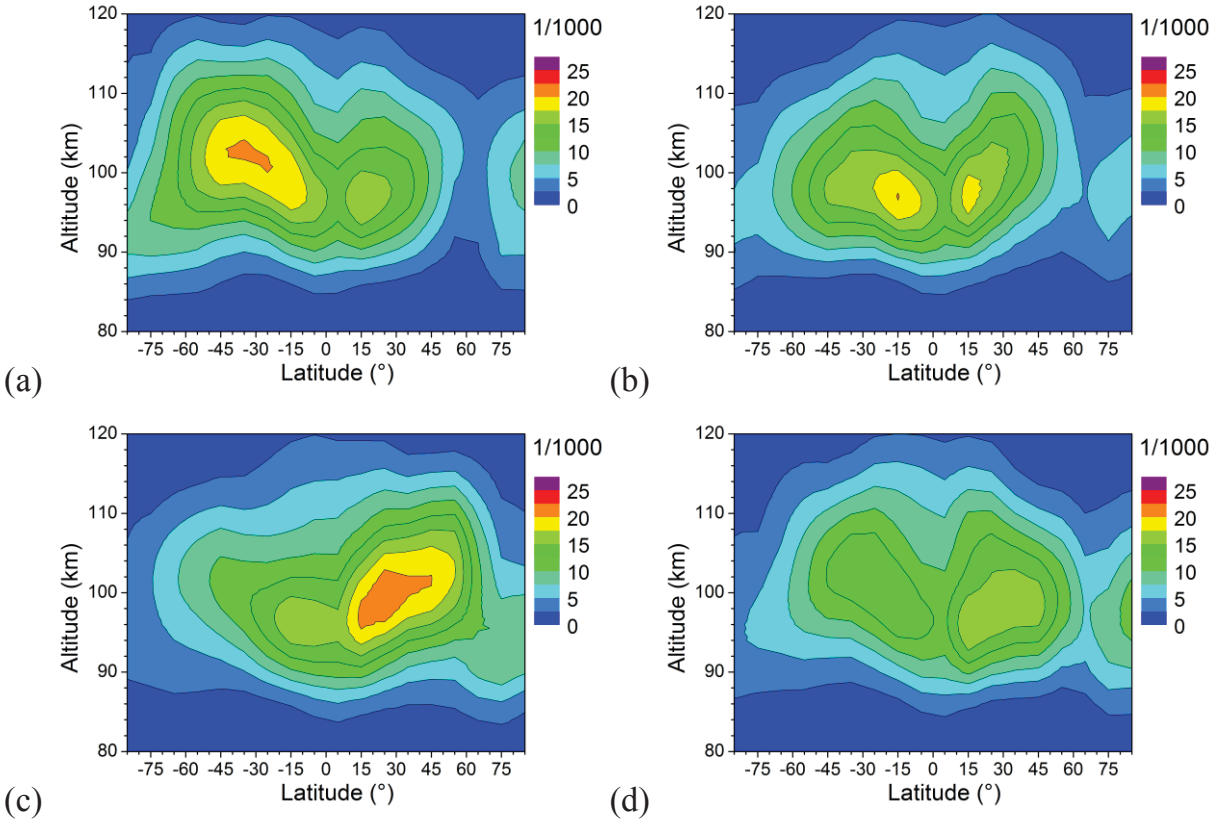

Fig. 1: 2007-2016 mean seasonal mean occurrence rates (a) DJF (b) MAM (c) JJA (d) SON.

3. QDT amplitudes in sporadic E occurrence rates.

In order to analyse the QDT signature in RO E_s, we sampled the detected E_s in a given latitudinal belt and height range according to local time, with a chosen time interval of one hour and a height range of 10 km. As with the global E_s OR, we divided the respective number of E_s by the number of RO in the time and latitude interval under consideration to obtain the OR. As an example, we show in Figure 2 the JJA diurnal

time-height distribution of OR for a latitude of 45 ± 5°N. We note the downward propagation of E_s OR signals, which are dominated by the SDT and, to a lesser degree, by a diurnal variation (see, e.g. Arras et al., 2009). Note that only migrating signatures, which are westward propagating with the sun, are visible in Figure 2 because we did not distinguish between latitudes in our analysis.

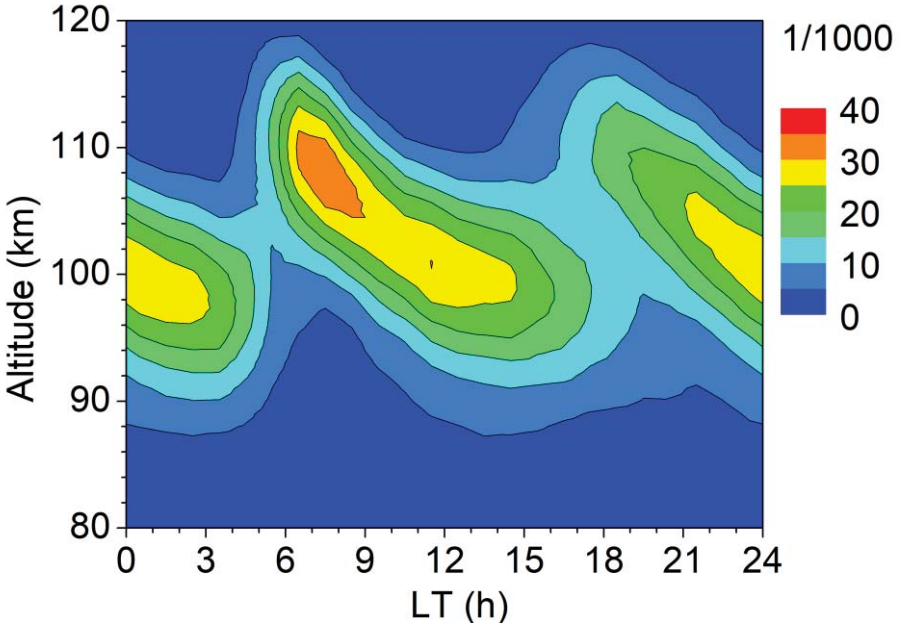

Fig. 2: Diurnal variation of E_s OR at 45 ± 5°N during summer (June-August, JJA). The OR in height gates of 10 km have been sampled, and the data have been attributed to the middle of the respective height interval.

In order to visualise the QDT component in E_s OR, we performed, for each altitude level separately, a multiple least-squares fit and analysed the respective 8-, 12-, and 24-h oscillation, which was then subtracted from the data exemplarily shown in Figure 2. The residual E_s OR for the same season and latitude as in Figure 2 are shown in Figure 3. A clear QDT component is now visible. The QDT phases, i.e. the times of maximum E_s OR for each altitude, are added as squares, while solid symbols denote significant amplitudes according to a t-test. These phases have been obtained from least-squares fitting analyses including the 6, 8, 12-, and 24 hr component. There is a downward phase progression, which is expected for the signature of a wave with upward energy flux.

The least-squares fit analyses of the QDT and the lower harmonics were then performed for each latitude between 85°S and 85°N in steps of 10°, and the results are shown in Figure 4. The amplitudes become small and irregular at low altitudes. Therefore, we present the data from 85 km onwards only. We note maximum amplitudes at midlatitudes with a maximum around 45°. In SON, the main maximum is however found at lower latitudes.

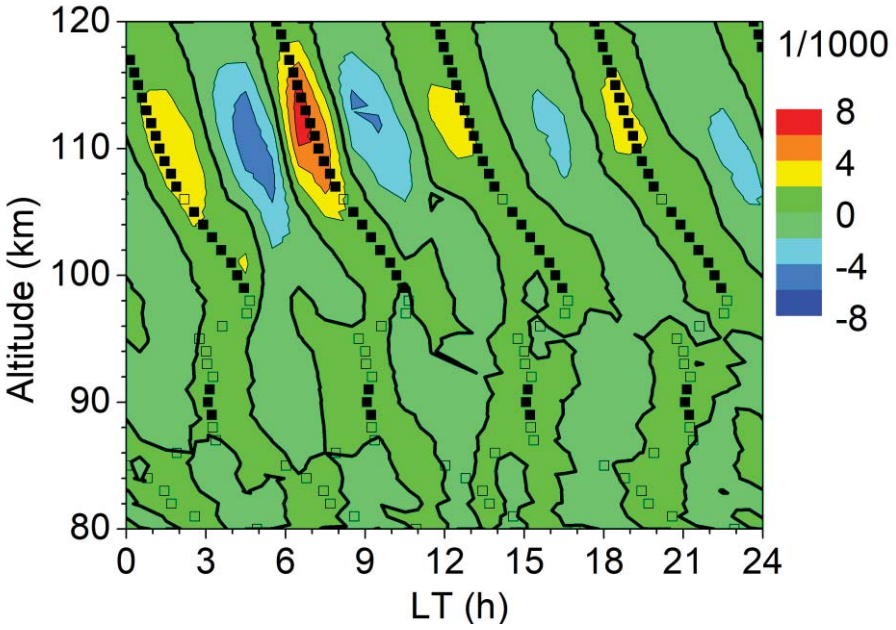

Fig. 3: JJA mean diurnal variation of E_s OR at 45 ± 5°N, after removing the 8, 12, and 24-hr components (contour lines). The QDT phases (times of maximum E_s OR) are added as squares. Solid symbols denote amplitudes significant at the 95% level according to a t-test.

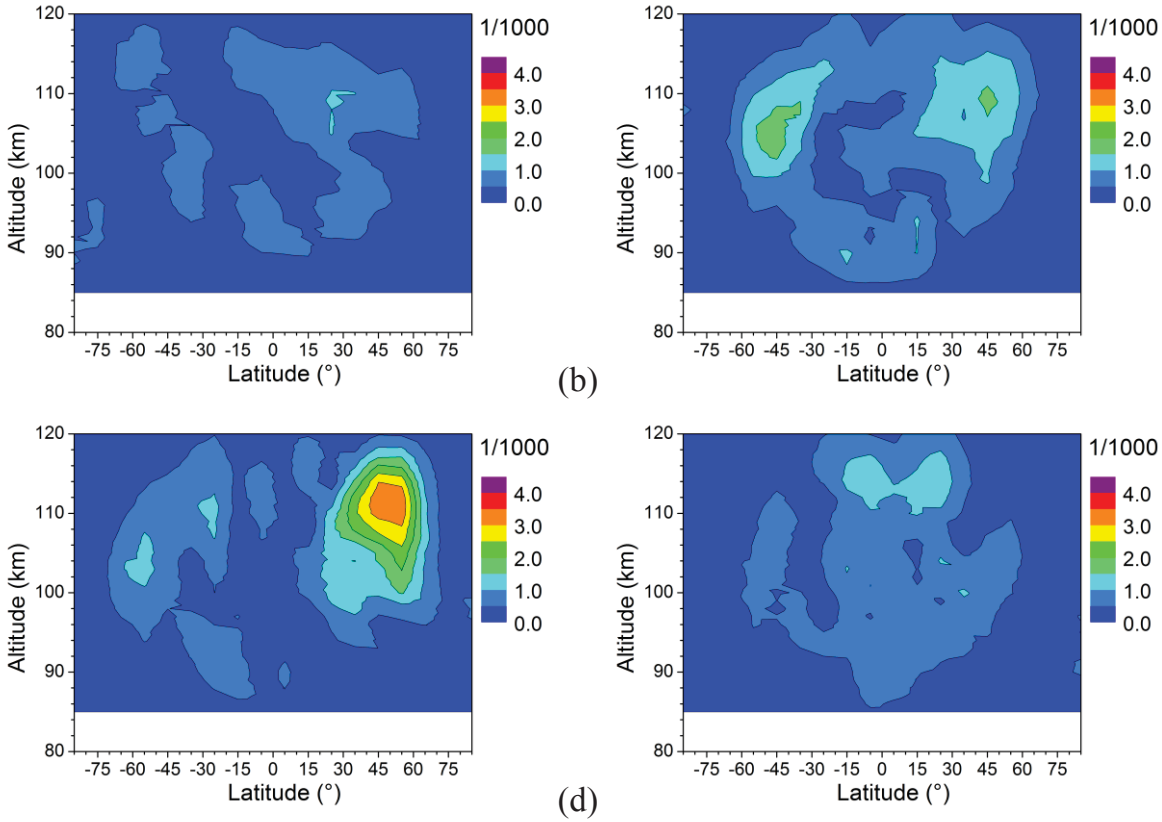

Fig. 4: 2007-2016 mean seasonal mean QDT amplitudes of E_s occurrence rates (a) DJF (b) MAM (c) JJA (d) SON.

4. Global distribution of QDT relative occurrence rate amplitudes

In Figure 3 and Figure 4, large QDT amplitudes are seen at altitudes between approximately 105 and 115 km. However, this does not necessarily reflect the distribution of the underlying tidal wave itself, because the OR amplitudes include both the dynamics, i.e. the 6 hr E_s signature production through QDT wind shear, and the background E_s OR, which is also influenced by background ionization, distribution of meteor rates (Haldoupis et al., 2007), and wind shear through other dynamical parameters. Therefore, to provide a better representation of the QDT, we divided the QDT amplitudes presented in Figure 4 by the background E_s OR shown in Figure 1 to obtain relative amplitudes, similar to the procedure described in Fytterer et al. (2014). These relative values are expected to more directly reflect the effect of the tides. Figure 5 shows the seasonal mean relative QDT amplitudes of E_s RO. The main difference to Figure 4 is that amplitudes in Figure 5 more strongly increase with altitude throughout the height range under investigation, which is more representative for a tide than a maximum at relatively low altitudes.

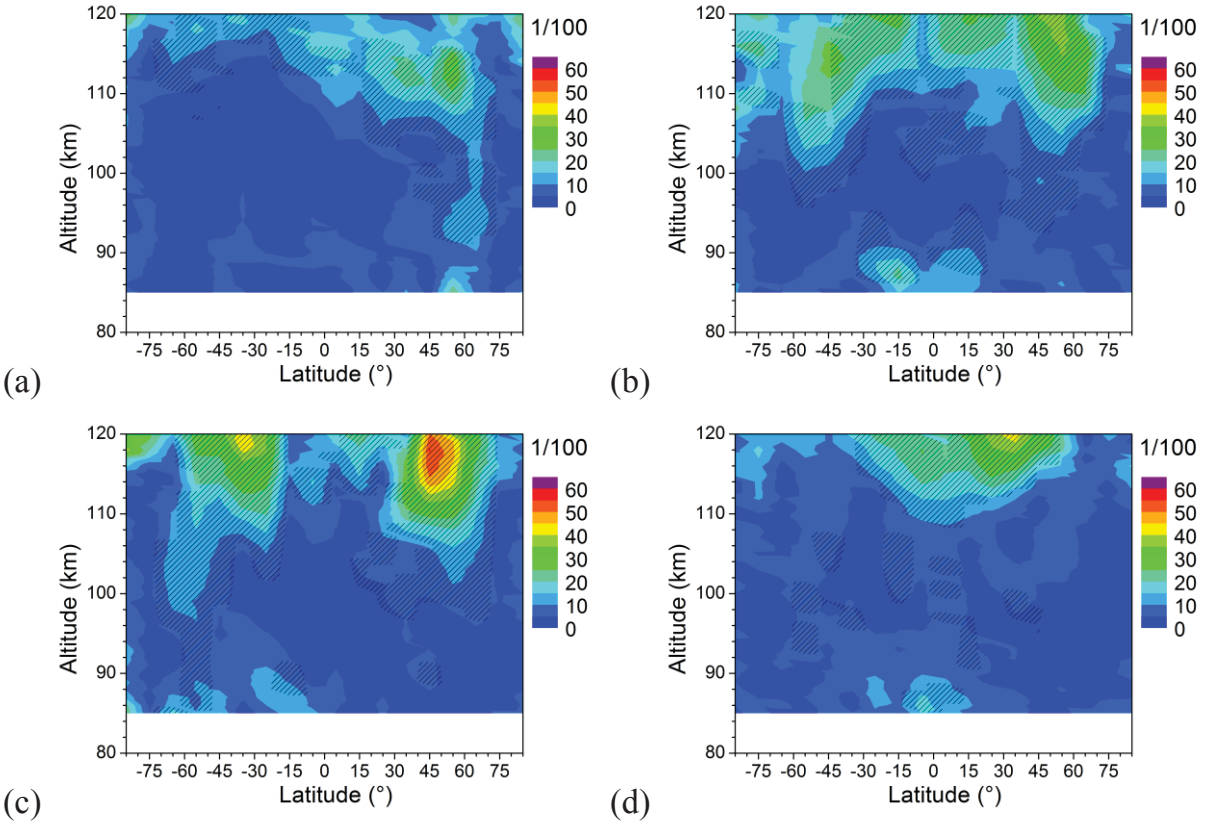

Fig. 5: 2007-2016 mean seasonal mean QDT relative amplitudes of E_s occurrence rates (a) DJF (b) MAM (c) JJA (d) SON. Values that are significant at the 95% according to a t-test are hatched.

The seasonal variation of E_s OR relative QDT amplitudes is shown in Figure 6 for 2 different heights. In contrast to the seasonal means presented above, mean relative amplitudes have been calculated here for each month. The figure shows that maximum relative amplitudes are seen at middle latitudes in both hemispheres, which is consis-

tent with SABER analyses of the QDT in temperature by Liu et al. (2015). At 95 km, there is a tendency for the QDT signature to maximize in the respective winter hemisphere. This has also been modelled by Smith et al. (2004), and is also seen in local radar observations at midlatitudes (Jacobi et al., 2017). At greater altitudes, the winter maxima are still visible. However, there is a strong summer maximum also, which only appears in the northern hemisphere.

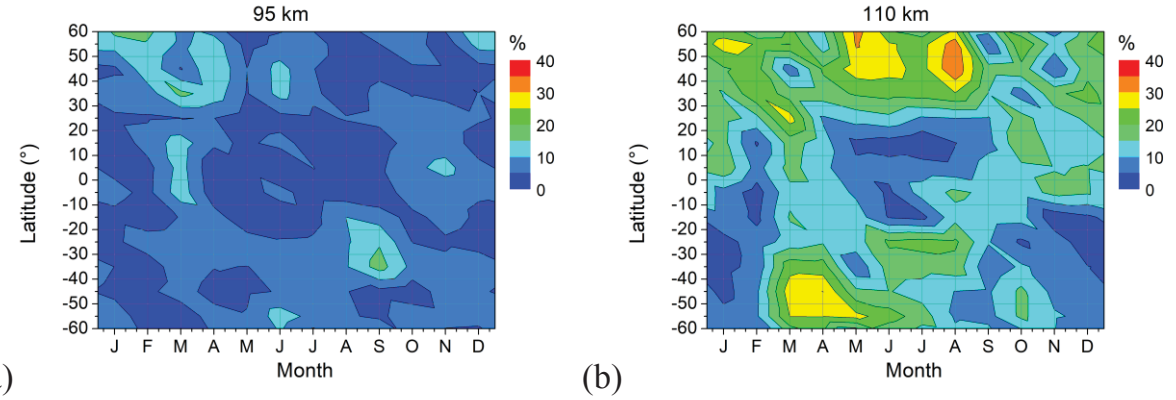

Fig. 6: Seasonal variation of E_s OR relative QDT amplitudes for 2 heights. The amplitudes base on monthly values from 2007-2016.

5. Conclusions

Analysing E_s OR from FORMOSAT-3/COSMIC GPS RO allows us to show that there is, besides the known DT, SDT and TDT signatures, also a QDT signal in E_s. It shows a downward propagation of the phase, which is consistent with an upward energy flux of the tidal wave responsible for this component of E_s diurnal variability.

The global distribution of relative QDT amplitudes in E_s OR shows some features known for the QDT in neutral atmosphere parameters, in particular a winter maximum, which is well expressed especially in the southern hemisphere, and a summer minimum at southern latitudes. The latter, however, in the northern hemisphere is only seen at altitudes below 100 km, where the amplitudes are generally weak, and at greater heights there is a pronounced summer maximum which has not been reported from radar observations. Future analyses will have to include modelling of the QDT as well as the more detailed comparison of the E_s QDT with observations to shed light on this possible discrepancy.

Acknowledgements

The provision of FORMOSAT-3/COSMIC data by University Corporation for Atmospheric Research is gratefully acknowledged. Ch. Jacobi acknowledges support through the Deutsche Forschungsgemeinschaft (DFG) under grant JA 836/34-1. C. Arras acknowledges support by the DFG Priority Program DynamicEarth, SPP 1788.

6. References

Anthes, R. A., Bernhardt, P. A., Chen, Y., Cucurull, L., Dymond, K. F., Ector, S., Healy, S. B., Ho, S.-P., Hunt, D. C., Kuo, Y.-H., Liu, H., Manning, K., McCormick, C., Meehan, T. K., Randel, W. J., Rocken, C., Schreiner, W. S., Sokolovskiy, S. V., Syndergaard, S., Thompson, D. C., Trenberth, K. E., Wee, T.-K., Yen, N. L., Zhang, Z., 2008: The COSMIC/FORMOSAT-3 mission: early results, Bull. Am. Met. Soc., 89, 313–333, https://doi.org/10.1175/BAMS-89-3-313.

Arras, C., Wickert, J., Beyerle, G., Heise, S., Schmidt, T., Jacobi, Ch., 2008: A global climatology of ionospheric irregularities derived from GPS radio occultation, Geophys. Res. Lett., 35, L14809, https://doi.org/10.1029/2008GL034158.

Arras, C., Jacobi, Ch., Wickert, J., 2009: Semidiurnal tidal signature in sporadic E occurrence rates derived from GPS radio occultation measurements at midlatitudes, Ann. Geophys., 27, 2555–2563, https://doi.org/10.5194/angeo-27-2555-2009.

Arras, C., Wickert, J., Heise, S., Schmidt, T., Jacobi, Ch., 2010: Global sporadic E signatures revealed from multi-satellite radio occultation measurements, Adv. Radio Sci., 8, 225–230, https://doi.org/10.5194/ars-8-225-2010.

Arras, C., Wickert, J., Jacobi, Ch., Beyerle, G., Heise, S., Schmidt, T., 2013: Global sporadic E layer characteristics obtained from GPS radio occultation measurements. In: Lübken, F.-J. (Ed.): Climate and Weather of the Sun-Earth System (CAWSES), Springer, Berlin, 207–222.

Arras, C., Wickert, J., 2017: Estimation of ionospheric sporadic E intensities from GPS radio occultation measurements, J. Atmos. Sol.-Terr. Phys., https://doi.org/10.1016/j.jastp.2017.08.006.

Bishop, R. L., Earle, G. D., 2003: Metallic ion transport associated with midlatitude intermediate layer development, J. Geophys. Res., 108, A11019, https://doi.org/doi:10.1029/2002JA009411.

Fytterer, T., Arras, C., Jacobi, Ch., 2013: Terdiurnal signatures in sporadic E layers at midlatitudes, Adv. Radio Sci., 11, 333–339, https://doi.org/10.5194/ars-11-333-2013.

Fytterer, T., Arras, C., Hoffmann, P., Jacobi, Ch., 2014: Global distribution of the migrating terdiurnal tide seen in sporadic E occurrence frequencies obtained from GPS radio occultations, Earth, Planets and Space, 66:79, https://doi.org/10.1186/1880-5981-66-79.

Hajj, G., Kursinski, E., Romans, L., Bertiger, W., Leroy, S., 2002: A technical description of atmospheric sounding by GPS occultations, J. Atmos. Sol. Terr. Phys. 64, 451–469, https://doi.org/10.1016/S1364-6826(01)00114-6.

Haldoupis, C., Meek, C., Christakis, N., Pancheva, D., Bourdillon, A., 2006: Ionogram height-time-intensity observations of descending sporadic E layers at mid-latitude, J. Atmos. Solar-Terr. Phys., 68, 539–557, https://doi.org/10.1016/j.jastp.2005.03.020.

Haldoupis, C., Pancheva, D., Singer, W., Meek, C., MacDougall, J. 2007: An explanation for the seasonal dependence of midlatitude sporadic E layers. J. Geophys. Res. 112, A06315, https://doi.org/doi:10.1029/2007JA012322.

Jacobi, Ch., Krug, A., Merzlyakov, E., 2017: Radar observations of the quarterdiurnal tide at midlatitudes: Seasonal and long-term variations, J. Atmos. Sol.-Terr. Phys., 163, 70–77, https://doi.org/10.1016/j.jastp.2017.05.014.

Kursinski, E. R., Hajj, G., Hardy, K. R., Schofield, J. T., Linfield, R., 1997: Observing the Earth's atmosphere with radio occultation measurements using the Global Positioning System, J. Geophys. Res., 102, 23429–23465, https://doi.org/10.1029/97JD01569.

Liu, M. H., Xu, J. Y., Yue, J., Jiang, G. Y., 2015: Global structure and seasonal variations of the migrating 6-h tide observed by SABER/TIMED, Science China: Earth Sciences, 58, 1216, https://doi.org/10.1007/s11430-014-5046-6.

Mathews, J. D., 1998: Sporadic E: current views and recent progress, J Atmos, Solar-Terr. Phys. 60, 413–435. https://doi.org/10.1016/S1364-6826(97)00043-6.

Morton, Y. T., Mathews, J. D., Zhou, Q., 1993: Further evidence for a 6-hr tide above Arecibo, J. Atmos. Terr. Phys, 55, 459–465, https://doi.org/10.1016/0021-9169(93)90081-9.

Smith, A. K., Pancheva, D. V., Mitchell, N. J., 2004: Observations and modeling of the 6-hour tide in the upper mesosphere, J. Geophys. Res., 109, D10105, https://doi.org/10.1029/2003JD004421.

Tong, Y., and Mathews, J. D., 1988: An upper E region quarterdiurnal tide at Arecibo? J. Geophys. Res., 93, 10,047–10,051, https://doi.org/10.1029/JA093iA09p10047.

Warburton, R. J., Goodkind, J. M., 1977: The influence of barometric-pressure variations on gravity, Geophys. J. R. Astr. Soc., 48, 281-292, https://doi.org/10.1111/j.1365-246X.1977.tb03672.x.

Whitehead, J., 1961: The formation of the sporadic E layer in the temperate zones, J. Atmos. Terr. Phys., 20, 49–58, https://doi.org/10.1016/0021-9169(61)90097-6